Simulation of X-Ray CT: Forward and Inverse Problems

Mustafa Alp Ekici
Electrical and Electronics Engineering
Middle East Technical University
Ankara, Turkey
Student ID: 2521524

***Abstract*—This term project focuses on the implementation and assessment of fundamental algorithms of X-Ray Computed Tomography (CT). These algorithms consist of two stages. These stages are forward projection and image reconstruction. For the forward problem, synthetic sinograms are created using the pixel grid. In particular, this is done by using a ray driven Exact Path Length method which calculates accurate intersection lengths on the pixel grid, thereby circumventing interpolation artifacts, and avoiding interstitial grid issues. For the inverse problem, the blurring limitation of Unfiltered Backprojection (UBP) is examined. A ray driven Filtered Backprojection (FBP) approach using the Ram-Lak filter in the frequency domain is utilized. The techniques are implemented on basic phantoms. As for the MSE, it was illustrated that under sufficient angular and spatial sampling, FBP decreases reconstruction error by nearly 80% compared to UBP.**

***Index Terms*—Computed Tomography, Radon Transform, Filtered Backprojection, Ray-Driven Algorithm, Medical Imaging, Image Reconstruction.**

I. Introduction

The ability to visually observe internal biological structures has greatly changed how people diagnose illnesses within medicine. Among all currently available imaging technologies, X-ray computed tomography (CT) imaging stands out above the rest due to its ability to provide high quality cross-sectional images, removing the depth ambiguity associated with traditional planar radiographs.

Johann Radon established the theoretical foundation of tomographic imaging in 1917. He proved that an infinite number of line integrals could be used to uniquely reconstruct a two-dimensional function [1]. Although Radon's theory was developed in the 1910s, CT technology wasn't put to use until the 1970s. During this period, Godfrey Hounsfield invented the first clinical CT scanner. He was later awarded the Nobel Prize for this outstanding accomplishment.

This project presents a comprehensive simulation of X-ray Computed Tomography in the MATLAB environment. The work involves two main computational areas. The first area is the Forward Problem, which creates projection data by modeling the physics of X-ray propagation through an object. This process is mathematically the same as the Radon Transform. The second domain is the Inverse Problem, which focuses on image reconstruction from these projections. Since reconstruction is a poorly defined problem, special editing techniques and filtering methods are required to recover the original attenuation distribution $\mu(x, y)$ with high accuracy [4].

II. The Forward Problem

In CT, the forward problem refers to generating projection data from a given digital image. Starting from a known attenuation map, the measurement process of a CT scanner is simulated by calculating detector values for several projection angles. The output is a series of projections (sinograms) representing the data acquisition phase of a real CT system.

A. Physical Principles

The physical basis of X-ray imaging rests on the Beer-Lambert law, which states that a monochromatic X-ray beam weakens exponentially when passing through a material [2]. If an X-ray beam with initial intensity I_0 traverses a path L, the detected intensity I is given by:

$$I = I_0 \exp\left(-\int_L \mu(x, y)\, ds\right) \tag{1}$$

where $\mu(x, y)$ is the linear attenuation coefficient of the material at spatial location (x, y). In CT, we are interested in the total attenuation which allows us to linearize the problem.

B. The Radon Transform

In a parallel-beam geometry, a projection profile at a specific angle θ consists of a set of line integrals. The path of each ray is parameterized by its perpendicular distance t from the origin. The coordinate transformation between the image frame (x, y) and the rotated projection frame t is:

$$t = x \cos\theta + y \sin\theta \tag{2}$$

Thus, the projection function $p_\theta(t)$ can be mathematically expressed as the Radon Transform of $\mu(x, y)$ [3]:

$$p_\theta(t) = \iint_{-\infty}^{\infty} \mu(x, y)\, \delta(x \cos\theta + y \sin\theta - t)\, dx\, dy \tag{3}$$

C. Algorithmic Implementation: Ray-Driven Approach

The projection algorithm makes it possible to convert the mathematical model of the Radon Transform into a discrete algorithm in MATLAB. The process begins with $\mu(x, y)$, which is the known attenuation coefficient distribution of the object. The algorithm assumes a parallel ray geometry and

generates a projection matrix for a specified number of rays and angular steps.

To do this, a coordinate system is defined based on the diagonal dimension of the object to ensure that it is fully covered. The primary technique used in this process is Ray-Driven. For each projection angle, θ, and each position of the detector t, the algorithm uses the equation of a line, $x\cos\theta + y\sin\theta = t$ to determine the precise position of the intersection of the X-ray beam and the grid of pixels that separate the mesh. The algorithm determines all possible entry and exit points of the pixels that the ray will cross, passing the rays in one direction and then the other by setting a particular value for x to find the corresponding value of y and then following the same method for y to find x.

After calculating these intersection points, values outside the physical limits of the object are removed. The valid points are sorted along the ray path. The algorithm computes the Euclidean distance for each consecutive pair of points to obtain the length of the ray segment in each individual pixel. Finally, to compute the total attenuation for that beam, the product of the pixel's attenuation value and this length of segment is calculated and all the products are summed.

D. Forward Projection Results

To confirm the correctness of the forward projection algorithm, it was tested on two different images. One was a simple square image, and the other was a more complex Shepp-Logan image.

1) Simple Square Image: First, the algorithm was tested using a 50×50 image containing a white square on a black background, as shown in Fig. 1.

Fig. 2 contains the projection profile for 101 beams for the values of the angles $\theta = 30°, 60°, 90°$, and $135°$ degrees. The profiles align with geometric expectations. For example, for $\theta = 90°$ degrees, the line equation $x\cos\theta + y\sin\theta = t$ simplifies to $y = t$. In this image the square is centered around $y = 10$, so rays with $t \approx 10$ go through the square and give a positive sum, while rays with t far from 10 miss the object and the value is zero. Because the line length through the square is constant for these vertical rays, $p(t)$ stays roughly flat on a short interval around $t = 10$ and zero elsewhere, so the projection profile looks like a rectangle.

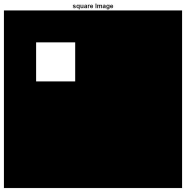

Fig. 1: Original Square Image

2) Shepp-Logan Image: To test the algorithm on a more intricate structure simulating human tissue, the Shepp-Logan image was used. The original image is shown in Fig. 3.

Fig. 4 shows the projection profiles obtained for the Shepp-Logan image. In contrast to projections on a simple square,

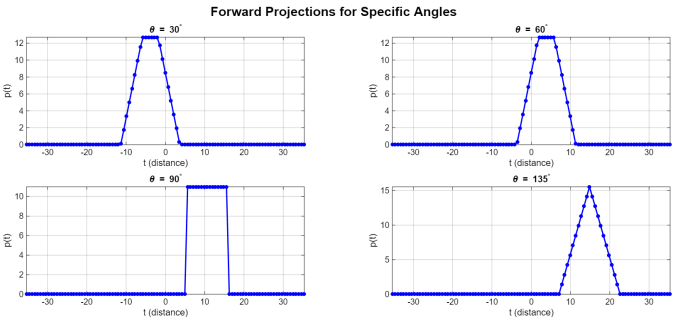

Fig. 2: Calculated projection profiles for Square Image

projections with more wavy and irregular shapes were observed. The projections reflect the gradual tissue variations in the image and the corresponding diverse attenuation.

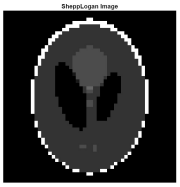

Fig. 3: Original Shepp-Logan Image

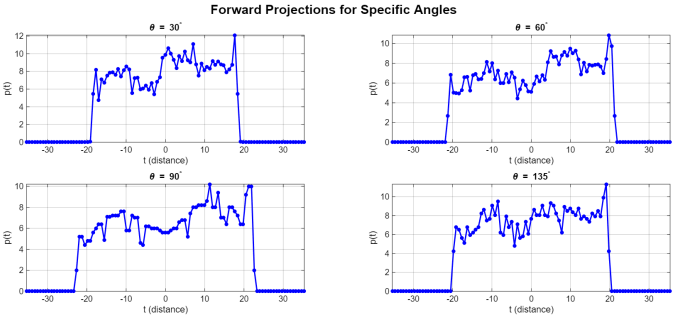

Fig. 4: Calculated projection profiles for Shepp-Logan Image

III. The Inverse Problem

The inverse problem is the reconstruction of an image from its projections. This is the computational core of a CT scanner.

A. Unfiltered Backprojection (UBP)

The simplest way to reconstruct the image is to reverse the projection process. Geometrically, this means that each projection profile is smeared back across the image plane along the image plane in the direction of the projection angle. Mathematically, Backprojection is defined as:

$$f_{UBP}(x,y) = \int_0^{\pi} p_\theta(x\cos\theta + y\sin\theta)\, d\theta \tag{4}$$

UBP is theoretically unsuitable for full reconstruction. It produces a blurred representation of the original object. The impulse response of the backprojection is proportional to

$1/r$, where r is the distance from the point source. This blurring makes UBP unsuitable in clinical diagnoses where edge sharpness is critical [5].

B. Filtered Backprojection (FBP)

Because of oversampling low frequencies, Unfiltered Backprojection naturally introduces blurring errors of $1/\rho$. To solve this problem, a Ram-Lak filter ($H(w) = |w|$), which acts as a high-pass filter to recover edge details in the frequency domain, was used.

First, the Fast Fourier Transform (FFT) of each projection profile $p_\theta(t)$ is calculated, and then the result is multiplied by the filter response.

$$P_{\theta,filt}(w) = P_\theta(w) \cdot |w| \tag{5}$$

Next, the filtered data is subjected to an IFFT process and projected back onto the image grid. This process removes blur and sharply reconstructs the original object.

C. Algorithmic Implementation of Reconstruction

The reconstruction algorithm was designed to be separate from the forward simulation to prevent the possibility of the "Inverse Crime". An inverse crime occurs when the exact same discrete matrix model is used for both data generation and inversion. This is often the case when errors are present and are low for no reason. To avoid this situation, the reconstruction grid is defined purely based on the output sizes and the projection data.

The Ray-Driven methodology located at the center of backprojection employs the Exact Integration technique. This technique is identically consistent with the Forward Projection technique and maintains the same geometric consistency between the data generation and reconstruction phases. For each projection angle θ and each t, the algorithm specifies an X-ray pathway and registers its precise intersection with each vertical and horizontal line in the reconstruction matrix. By computing the Euclidean distance between intersections, the algorithm determines the precise path length (segment length, L) that the ray traverses in each individual pixel. This value is used as a weight to transfer to the appropriate pixel the value of the filtered projection (val_{filt}) as follows $Pixel(x, y) = Pixel(x, y) + (val_{filt} \times L)$. In contrast to the pixel driven approach where pixels are treated as indivisible mathematical points, this approach is more refined as it accurately models the pixel grid.

D. Reconstruction Results

Three separate datasets were used to assess the reconstruction algorithm's effectiveness. These datasets were used to demonstrate the algorithm's strength against various geometries: a standard Offset Square to assess edge response, a Radial Star to check for angular resolution, identification of high frequency components, and Horizontal Strips to measure contrast resolution at different levels of intensity. In all of the simulations, high resolution parameters were chosen in order to limit the amount of sampling artifacts. This was accomplished using a total of 201 beams for every projection and an angular step of 1 degree (resulting in 180 projections).

This dataset shows striking differences between methods in visual reconstruction. The Offset Square (Fig. 5) has UBP exhibiting the low frequency "foggy" effect, whereas the Filtered Backprojection (FBP) successfully recovers the square with sharp edges and uniform interior intensity. This effect can also be seen in the Radial Star dataset (Fig. 6), where the geometry looks difficult, with narrow, sharp converging points. UBP is unable to resolve the center of the star and its arms, while FBP captures the tips perfectly. There is no loss of resolution as the star arms are crisply defined. This also holds in Strips (Fig. 7), where the FBP reconstruction of adjacent regions shows no bleeding, along with several distinct gray levels differing considerably. This shows the algorithm resolves contrast effectively.

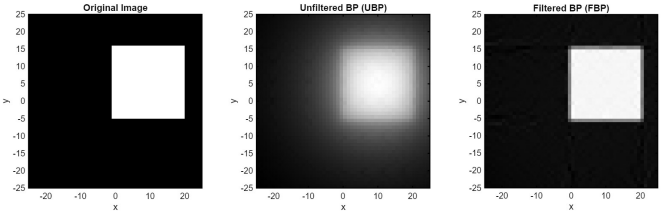

Fig. 5: Reconstruction Results for Offset Square. (Left) Original Image, (Center) UBP, (Right) FBP.

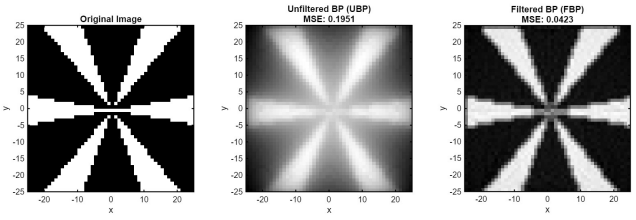

Fig. 6: Reconstruction Results for Radial Star. (Left) Original Image, (Center) UBP, (Right) FBP.

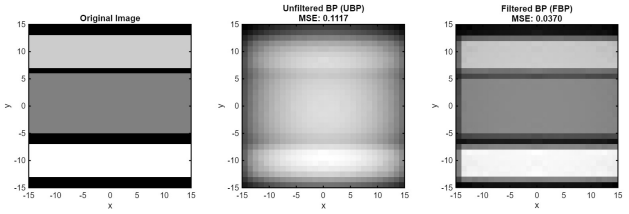

Fig. 7: Reconstruction Results for Intensity Strips. (Left) Original Image, (Center) UBP, (Right) FBP.

IV. Quantitative Analysis

A. Mean Squared Error (MSE) Comparison

To objectively evaluate image quality rather than relying solely on visual inspection, a metric called Mean Squared Error (MSE) has been chosen to measure image quality. MSE calculates the average of the square of the errors. This means that the mean squared difference between the estimated value and the actual value is evaluated. In this project, MSE evaluates the pixel deviation between the reconstructed images and the actual images (ground truth) obtained from phantoms. To enable scale-independent comparisons, both the reconstructed images and the corresponding actual images were normalized between 0 and 1 in each iteration of this project.

$$MSE = \frac{1}{MN} \sum_{i,j} (I_{orig}(i,j) - I_{recon}(i,j))^2 \qquad (6)$$

Table I summarizes the results. The FBP algorithm consistently reduces the error by a factor of 4 to 5 (approx. 80% reduction) compared to UBP. The remaining error in FBP is largely due to the discretization of the Radon transform (finite number of rays and angles), which inevitably introduces some aliasing.

TABLE I: Quantitative Comparison of Reconstruction Methods (201 Beams, 1° Step)

Test Image	UBP MSE	FBP MSE	Error Reduction
Offset Square	0.0526	0.0106	**79.8%**
Radial Star	0.1951	0.0423	**78.3%**
Strips	0.1117	0.0370	**66.9%**

B. Sensitivity Analysis

To understand the trade-offs in CT system design, the reconstruction quality was analyzed under different sampling conditions (Table II).

TABLE II: Effect of Sampling Parameters on Image Quality

Case	Beams	Angle Step	Total Proj.	FBP MSE
Low Spatial	100	1°	180	0.0274
Low Angular	201	5°	36	0.0159
Reference	201	1°	180	0.0095

V. Discussion

In the forward problem, projection data quality is mainly determined by sampling. Detector axis spatial sampling is determined by the number of beams. Using too few beams causes projection profiles to become coarse, resulting in insufficient capture of high-frequency details, like sharp edges. The angular step size controls the angular sampling. Large angular steps lead to angular undersampling in the Radon domain, which creates artifacts in the sinogram, while smaller angular steps create a sinogram with a smoother appearance, but at the cost of higher computational load.

In the inverse problem, the results give insight into the main disadvantage of Unfiltered Backprojection (UBP): during backprojection the contrast at the edges is lost. This diminishes edge clarity. Filtered Backprojection (FBP) addresses this problem through the use of the Ram-Lak filter, in which the low-frequency components are suppressed before backprojection through a frequency weighting function. This indeed reduces the low-frequency blurring and improves edge contrast, and thus is evidenced in the case of the Mean Squared Error (MSE) where FBP has far lower error values than UBP. It is important to state that although the Ram-Lak filter increases resolution in this noise-free simulation, in real world measurement situations, it tends to increase the level of high-frequency noise.

VI. Conclusion

This study describes the successful implementation and evaluation of the primary computational stages of X-ray Computed Tomography (CT), specifically forward projection and image reconstruction. Using the Ray-Driven algorithm with Exact Path Length computation, the physical principles of X-ray attenuation were accurately modeled to generate consistent sinograms for various phantoms.

The comparative analysis between Unfiltered Backprojection (UBP) and Filtered Backprojection (FBP) demonstrated the critical importance of frequency domain filtering in tomographic imaging. While the UBP generated blurred images as a result of the backprojection operator's direct response of $1/r$, FBP recovers high-frequency components and sharpens edges compared to UBP. The quantitative result also justified the FBP as it generated a mean squared error (MSE) of 80% lower than that of the UBP in all of the test geometries.

Moreover, the sensitivity analysis showed the relationship between sampling parameters and quality of reconstruction. It was observed that there were significant aliasing artifacts when there was insufficient sampling either spatially or angularly which showed the balance between the constraints of the data acquisition and the quality of the image. Consequently, this project validates that accurate CT reconstruction requires not only robust filtering techniques but also optimized sampling strategies to minimize artifacts and maximize diagnostic value.

References

[1] A. C. Kak and M. Slaney, *Principles of Computerized Tomographic Imaging*. New York, NY: IEEE Press, 1988.

[2] J. L. Prince and J. M. Links, *Medical Imaging Signals and Systems*. Upper Saddle River, NJ: Pearson Prentice Hall, 2006.

[3] J. Hsieh, *Computed Tomography: Principles, Design, Artifacts, and Recent Advances*, 2nd ed. Bellingham, WA: SPIE Press, 2009.

[4] F. Natterer, *The Mathematics of Computerized Tomography*. Philadelphia, PA: SIAM, 2001.

[5] T. M. Buzug, *Computed Tomography: From Photon Statistics to Modern Cone-Beam CT*. Berlin, Germany: Springer, 2008.